Effect of Al Trace Dimension on Electromigration Failure Time of Flip-Chip Solder Joints

S.H. CHIU,[1] CHIH CHEN,[1] and D.J. YAO[2]

1.—National Chiao Tung University, Department of Materials Science & Engineering, Hsinchu 30050, Taiwan, R.O.C. 2.—National Tsing Hua University, Institute of Microelectromechanical System, Hsinchu 300, Taiwan, R.O.C.; e-mail: chihchen98@yahoo.com

The effect of Al-trace dimension on electromigration of flip-chip solder joints was investigated. The Al trace dimension was found to have a significant influence on the electromigration failure time. When joints with Al traces 100 μm wide were stressed by 1.0 A at 100°C, failure times were 35 h, 1,700 h, and >3,000 h for joints with Al traces that were 2,550 μm, 1,700 μm, and 850 μm long, respectively. Solder joints with Al traces 40 μm wide and 2,550 μm long failed instantly at 0.6 A. The Joule heating effect was found to be responsible for the huge difference in failure time.

Key words: Electromigration, flip chip, Joule heating

INTRODUCTION

To meet the miniaturization trend for portable devices, flip-chip technology has been adopted for high-density packaging due to its excellent electrical performance and better heat-dissipation ability.[1] As the required performance of microelectronics devices becomes higher, design rules require that the current in each bump be 0.2 A, and this value is expected to increase to 0.4 A in the near future.[2] Therefore, electromigration has become an important issue in reliability.[3–4] During the electromigration test, the applied current may be as high as 2.0 A; thus the Joule heating effect in the solder bumps becomes significant.[5] Furthermore, the total length of the Al trace ranges typically from a few hundred to a few thousand microns, which corresponds to a resistance of approximately a few hundred milliohms or several ohms. However, the resistances of the solder bumps and the Cu trace in the substrate are relatively low, typically about a few or tens of milliohms. The major heat source for the solder joints is the Al trace.[6] Hence, the temperature in the bumps during testing may be much higher than the ambient temperature, due to Joule heating, and this may affect the mean time-to-failure (MTTF) analysis, as delineated by the Black equation[7]:

$$\mathrm{MTTF} = A\frac{1}{j^n}\exp\left(\frac{Q}{kT}\right) \tag{1}$$

where A is constant, j is the current density, n is a model parameter for current density, Q is the activation energy, k is the Boltzmann constant, and T is the average bump temperature. It is noteworthy that the MTTF decreases exponentially with the stressing temperature. Wu et al.[8] conducted electromigration tests for SnPb solder bumps and found that the MTTF decreased from 711 h to 84 h when the testing temperature increased from 125°C to 150°C at 5.0×10^3 A/cm^2, whereas the MTTF decreased from 277 h to 84 h as the current density increased from 2.5×10^3 to 5.0×10^3 A/cm^2 at 150°C. Therefore, the influence of the stressing temperature on MTTF is more profound than that of the current density.

However, few investigations of the Joule heating effect in the solder joints during electromigration have been carried out. The solder joints are surrounded by a Si substrate, underfill, and a substrate; thus it is difficult to measure the temperature increase inside the solder joints. In this study, we use an infrared microscope to investigate the Joule heating effect in the solder joints with different Al trace dimensions. This study provides a better understanding on the effect of Al trace dimension on electromigration of solder joints.

EXPERIMENTAL PROCEDURES

The dimension of the flip-chip joint used in this study is shown schematically in Fig. 1a. The under bump metallization (UBM) was 0.5-μm Ti/0.5-μm Cu/5-μm Cu/3-μm Ni. The Ti layer and the 0.5-μm Cu seed layer were sputtered, whereas the 5-μm Cu and the 3-μm Ni layers were electroplated. The passivation and UBM openings are 110 μm and

(Received January 4, 2006; accepted May 5, 2006)

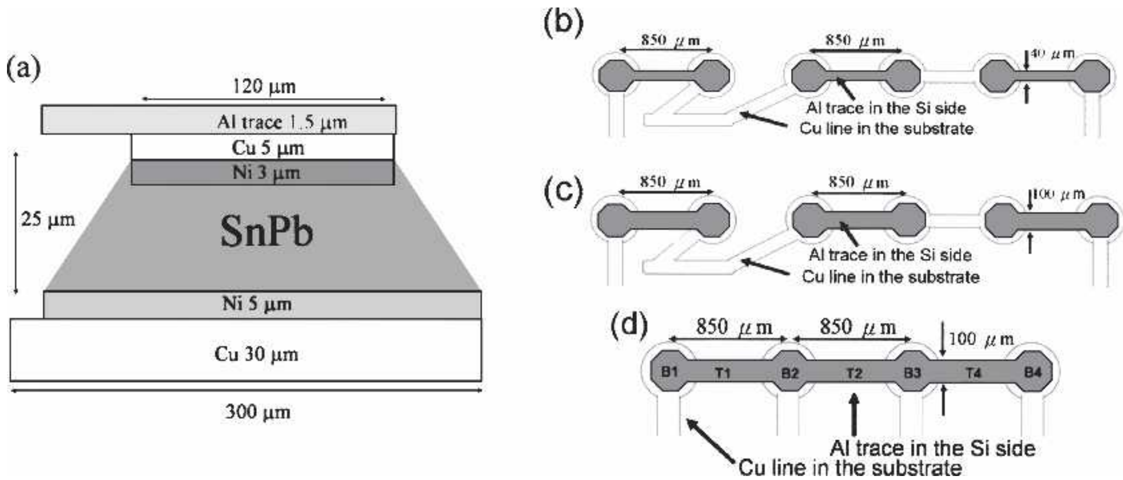

Fig. 1. Schematic diagrams of the samples used in this paper. (a) Cross-sectional view showing the materials and the dimension of a SnPb bump. (b) Plan-view schematic showing the daisy-chain joints with (b) 40 μm wide Al traces and (c) 100 μm wide Al traces. (d) Plan-view schematic showing the solder joints with 100 μm wide Al traces for investigation of length effect on electromigration.

120 μm in diameter, respectively. Eutectic SnPb solder was adopted, and the solder bumps were jointed to FR4 substrates. The dimension of the pad opening in the substrate was 300 μm in diameter. The dimension of the Si chip was 5.35 mm long, 4.35 mm wide, and 250 μm thick, whereas the dimension of the FR4 substrate was 5.35 mm long, 4.35 mm wide, and 250 μm thick. Three different layouts were fabricated, and the pitch for all the test samples was 850 μm. The first layout was 40 μm wide and 1.5 μm thick (Fig. 1b). The second layout was 100 μm wide and 1.5 μm thick (Fig. 1c). Both are daisy-chain structures with six bumps. Thus, they can be used to investigate the width effect of the Al trace on electromigration. The third layout is depicted in Fig. 1d, in which the four bumps were connected by three segments of Al traces. The four bumps in Fig. 1d are labeled as B1 through B4, the three Al traces are labeled as T1 through T3, and the four Cu lines/nodes in the FR4 substrate are labeled as N1 through N4. This layout is not a daisy-chain structure. Three experimental setups were used to examine the effect of length on electromigration: current was applied through N1 and N2, through N1 and N3, or through N1 and N4. All three of the stressing setups passed through two bumps but different lengths of Al traces. Thus, the effects of bump resistance and contact resistance could be excluded.

An infrared (IR) microscope was employed to measure the temperature in the Al trace during current stressing. The temperature distribution inside the bumps when powered by electric current was detected by a thermal IR microscope, which has the resolution of 0.1°C in temperature sensitivity and 2.8 μm in spatial resolution. The IR measurement was performed before the electromigration test. During the temperature measurement, the flip-chip package was placed on a hot stage maintained at 100°C, and the Si side faced the IR microscope. Because the 250-μm Si is transparent to infrared, the Al traces that are located between the Si and the solder joints are visible to the infrared microscope. Therefore, the temperature distribution in the Al traces and in the Al pad directly above the solder bumps during current stressing can be measured. Due to the large opening in the substrate side, the bump height was as small as 25 μm. Scanning electron microscopy (SEM) was used to observe the failure sites.

RESULTS AND DISCUSSION

Electromigration tests were performed for the solder joints described above to examine the effect of Joule heating on electromigration failure time. For the solder joints with the 40 μm wide Al trace, they failed instantly at and above 0.6 A at 100°C. The SnPb solder may be melted at these stressing conditions. Nevertheless, the failure time was 18 h when 0.6 A was applied to the solder joints with the 100 μm wide Al trace (Fig. 1b). For the solder joints with the 100 μm wide Al trace (Fig. 1d), electromigration failure time was 35 h when a current of 1.0 A was applied through bumps B1 and B4 at 100°C. The corresponding current density was 7.1×10^3 A/cm^2 on the basis of the UBM opening. However, when the same amount of current was applied through bumps B1 and B3, the failure time was 1,700 h. When the current was applied through bumps B1 and B2, the joints did not fail even after 3,000 h. Therefore, the dimension of the Al trace has a huge effect on the electromigration failure time. Table I summarizes these results. In addition, the failure modes for the above stressing conditions are quite similar. Figure 2 shows the cross-section scanning electron microscopy (SEM) image for the typical failure morphology. The failure always occurred in the bump with electron flow from chip side to the substrate side. The UBM layer was consumed, and voids formed near the chip side.

Because the current-density distribution was the same for the three stressing conditions for solder joints with the 100 μm wide Al trace, differences in failure time were attributed mainly to the differences

Table I. Failure Time of the Solder Joints with Various Al Trace Lengths under Current Stressing

Al trace dimension					
Length (μm)	850	1700	2550	2550	2550
Width (μm)	100	100	100	40 (daisy chains)	100 (daisy chains)
Applied current (A)	1.0	1.0	1.0	0.6	0.6
Failure time (h)	>3000	1700	35	Failed instantly	18

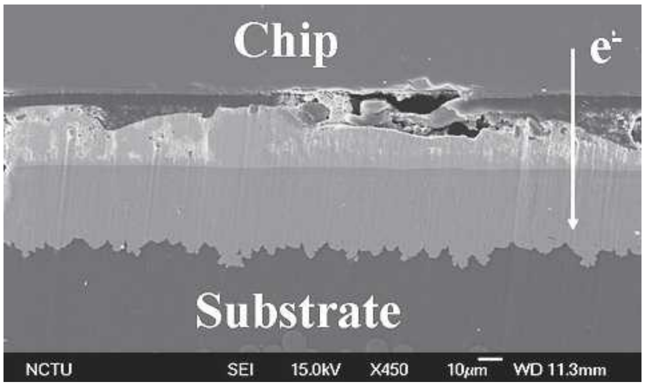

Fig. 2. Cross-sectional SEM image showing the typical failure mode for the samples used in this study.

in Joule heating effect. To examine the Joule heating effect in the solder joints, the temperature distribution in the Al trace and in the Al pad was measured using an IR microscope. Figure 3a shows the IR radiant image of the bump B1 with a 100 μm wide Al trace (Fig. 1d). The Al trace and Al pad can be clearly observed in the figure. Figure 3b shows the temperature distribution before the current stressing when the package was placed on a hot plate that was maintained at 100°C, in an air ambient. The temperature distribution was quite uniform. When the solder joint was stressed by the current, the temperature in the Al trace and in the Al pad can be measured based on the calibration in Fig. 3b. Figure 3c shows that the temperature increases in the Al pad for the bump B1 in Fig. 1d when stressed by 1.0 A through bumps B1 and B4. In this paper, the average temperature in the Al pad was obtained by averaging the temperatures in a square of 40 μm × 40 μm in the center of the pad (dotted lines in Fig. 3b). The average temperature increase due to the current stressing was as high as 65.1°C.

The Joule heating effect in the solder joints with different lengths of Al traces was investigated using the test structure in Fig. 1d. The current may be applied through bumps B1 and B2, through bumps B1 and B3, or through bumps B1 and B4. Thus, current flows through Al traces of T1, (T1 + T2), and (T1 + T2 + T3), respectively, for the above three current-stressing setups. The corresponding lengths of the Al traces are 850 μm, 1700 μm, and 2,550 μm, respectively. Figure 4 shows the temperatures in the Al pad of the bump B1 as a function of applied currents up to 1.0 A for the three stressing setups. At lower stressing currents below 0.2 A, there were no obvious differences in temperature for the three stressing conditions. However, temperature differences became more pronounced as the applied current was increased. When stressed by 1.0 A, the temperature in the pad was 119.1°C, 138.6°C, and 165.1°C for the three stressing setups, respectively. The differences are significant in terms of electromigration. Consequently, the Joule heating effect was the main reason behind the significant difference (as described above) in the electromigration lifetime under the same current.

On the other hand, the width of the Al trace may affect the Joule heating profoundly in solder joints at high stressing currents. To investigate the width effect, the current was applied through the far-left and far-right bumps in Fig. 1b, and the same amount of current was applied through the far-left and the far-right bumps in Fig. 1c. The temperatures in the Al pad of the far-left bumps of the two layouts were measured during current stressing. For both layouts, the Al trace was 2,550 μm long. The measured resistance values were 1.08 Ω and 2.66 Ω at 100°C for the layout with 100 μm and 40 μm wide Al traces, respectively. Figure 5 shows the temperatures in the far-left bumps as a function of applied current for solder joints with 40 μm and 100 μm wide Al traces. When a 0.2-A current was applied, the temperature difference was only 2.1°C between the two solder joints. However, it increased up to 20.1°C at 0.6 A. Therefore, the width of the Al trace also has a significant effect on Joule heating in solder joints.

The measured temperature on the Al pad may be close to the temperature of the solder bump located directly below it, as metals are good heat conductors and the total thickness of both Al and UBM is <10 μm. From analysis by a one-dimensional lumped model, the temperature difference between the Al pad and the top layer of solder was estimated to be only 0.5°C. Therefore, the measured temperatures in the Al pad are quite meaningful, and they could be used to investigate the Joule heating effect in the solder bumps.

The Joule heating effect is larger than expected. The heating power can be expressed as

$$P = I^2R \qquad (2)$$

where P is the Joule heating power, I is the current, and R is the resistance. The product I^2R is the total heating power. In this study, the total resistance was 1210 mΩ at 100°C for the stressing circuit in Fig. 1d when powered through bumps 1 and 4, in which the resistance of the Al trace was weighted at 81% of the total resistance of the stressing circuit.

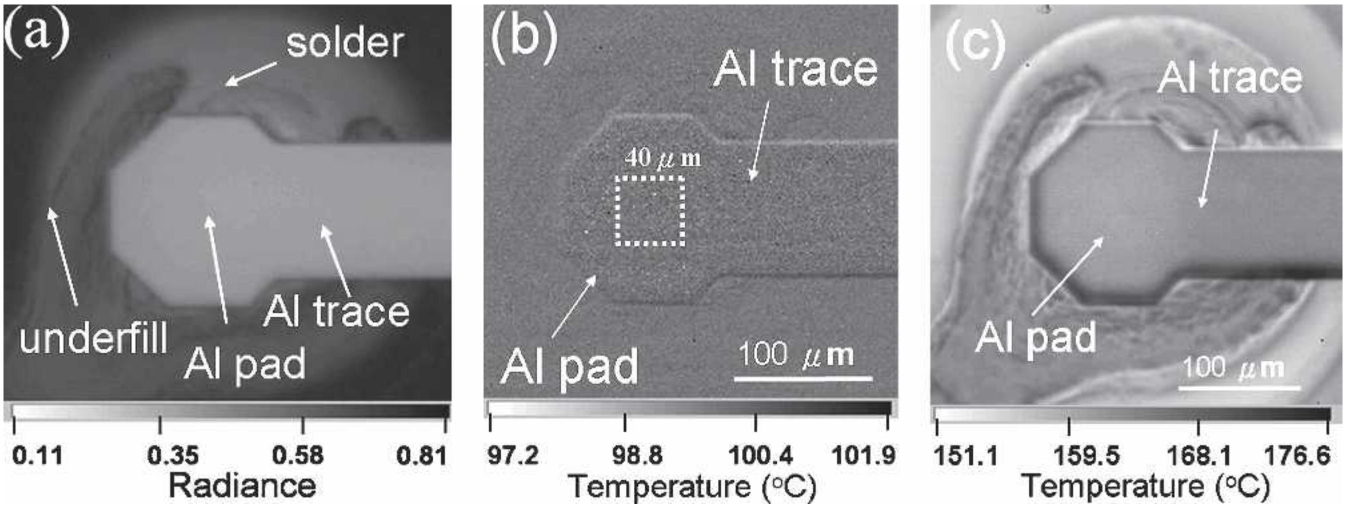

Fig. 3. (a) Radiant IR image showing bump B1 in Fig. 1d. The Al pad, underfill, and solder are observed clearly. (b) Uniform temperature distribution in the Al trace and in the Al pad before current stressing. The average temperature in the Al pad was obtained by averaging the temperatures in the 40 μm × 40 μm square. (c) Temperature distribution with 1.0-A current application.

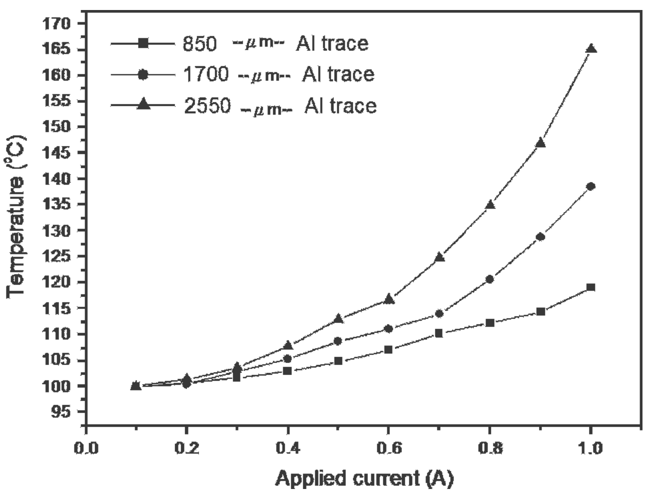

Fig. 4. Temperatures measured in the Al pad for solder joints with 850 μm, 1700 μm, and 2,550 μm long Al traces in Fig. 1d as a function of applied current. The longer the Al trace, the higher the Joule heating effect.

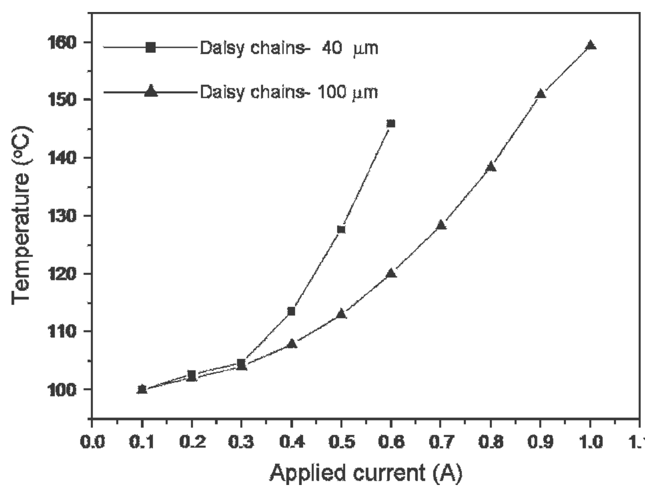

Fig. 5. Temperatures measured in the Al pad of the first bumps in Figs. 1b and c with the 2,550 μm long Al trace as a function of applied current.

The resistance of a solder bump is only about 5 mΩ,[9] and the rest of the resistance was contributed from the Cu line in the substrate. Consequently, the Al trace was the major heat source to influence the temperature in the solder bumps. Based on Eq. 2, the plot of temperature increase as a function of the square of the applied current is expected to be linear because the temperature increase is proportional to the heating power. However, the temperature increase was higher than the linear relationship. Figure 6 shows the plot of the measured temperature increase against the square of the applied current for the solder with the 2,550 μm long Al trace in Fig. 4. The dotted line in the figure was the tangent line for the fitted curve at zero applied current. It was found that, the higher the applied current, the greater the deviation of the temperature from the linear relationship. However, based on Eq. 2, the plot of the temperature increase against the square of the applied current should be linear (dotted line in Fig. 6). The deviation from the linear relationship may be mainly attributed to the temperature coefficient of resistivity (TCR). During the electromigration test at an elevated temperature, for example, 100°C, resistances of the Al, Cu, and solder increased due to the TCR effect. In addition, when high currents are applied, the Joule heating effect raises the temperatures of the Al traces, Cu lines, and solder bumps, increasing their resistances even higher. Thus, Eq. 2 should be modified to account for the TCR effect. Typically, the TCR can be assumed to be linear and can be expressed as

$$\rho(T) = \rho(T_0) \times [1 + a(T - T_0)] \qquad (3)$$

where a is the TCR, T is the test temperature, $\rho(T)$ is the resistivity at T (°C), and $\rho(T_0)$ is the resistivity at T_0 (°C). The TCR for bulk Al is 4.2×10^{-3} K^{-1}, and

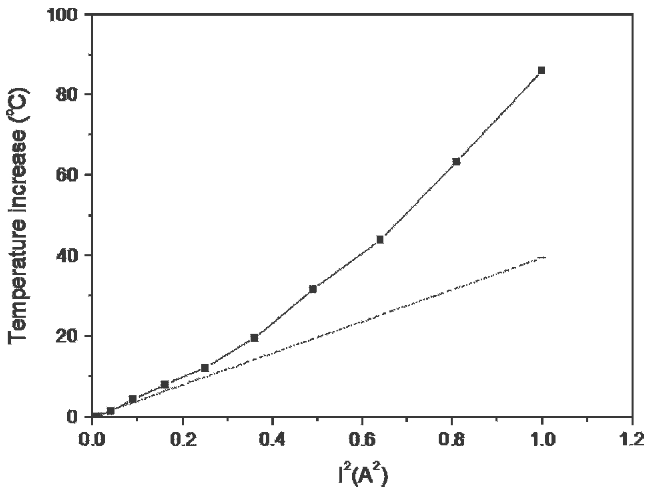

Fig. 6. Plot of temperature increase in the Al pad against the squares of the applied current (I^2), showing that the Joule heating effect was larger than was the I^2 dependence. The straight line is plotted using the first two points.

the resistivity for Al is 2.7 μΩ·cm at 20°C. However, it increases to 4.2 μΩ·cm at 100°C, which is a 55.6% increase. Consequently, the heating power at 150°C is ~1.5 times larger than that at 20°C under the same applied current. Hence, the heating power should be revised as

$$P = I^2R(T) = j^2V\{\rho(T_0) \times [1 + a(T - T_0)]\} \quad (4)$$

where j is current density and V is volume.

Thus, the temperature in the Al-pad during current stressing could be expressed as

$$T_{Al\ pad} = 100°C + dT = 100°C + I^2R(T)\theta \quad (5)$$

where the $T_{Al\ pad}$ is the temperature in the Al pad, dT is temperature increase due to the Joule heating effect, and θ is the thermal resistance. Therefore, the TCR has a significant influence on the Joule heating effect in flip-chip solder joints, and it enhances the Joule heating effect during accelerated electromigration test. Therefore, due to the serious Joule heating during accelerated electromigration tests, Black's equation cannot be applied to predict the MTTF of solder joints without calibrating the real temperature in the solder joints. On the other hand, our results indicate that the shortening and widening of the Al trace between the solder bumps may increase the electromigration lifetime.

CONCLUSIONS

The electromigration lifetime depends strongly on the dimensions of the Al trace. The dimensions of the Al trace were observed to play crucial roles in the Joule heating effect, as the Al trace is the major heating source. Under the same stressing currents, solder joints with longer Al traces had greater increases in temperature, and solder joints with 40 μm wide Al traces had higher Joule heating effects than did those with 100 μm wide Al traces.

ACKNOWLEDGEMENTS

The authors thank the National Science Council of R.O.C. for financial support (grant no. 94-2216-E-009-021).

REFERENCES

1. *International Technology Roadmap for Semiconductors, Assembly and Packaging Section* (San Jose, CA: Semiconductor Industry Association, 2003), pp. 4–9.
2. K.N. Tu, *J. Appl. Phys.* 94, 5451 (2003).
3. S. Brandenburg and S. Yeh, *Proc. Surface Mount International Conference and Exhibition, SMI 98*, San Jose, CA, Aug. 23–27, 1998 (Edina, MN: SMTA, 1998), p. 337.
4. C.Y. Liu, C. Chen, C.N. Liao, and K.N. Tu, *Appl. Phys. Lett.* 75, 58 (1999).
5. T.Y.T. Lee, T.Y. Lee, and K.N. Tu, *Proc. 51st Electronic Components and Technology Conference,* IEEE Components, Packaging, and Manufacturing Technology Society (Piscataway, NJ: IEEE, 2001), p. 558.
6. T.L. Shao, S.H. Chiu, C. Chen, D.J. Yao, and C.Y. Hsu, *J. Electron. Mater.* 33, 1350 (2004).
7. J.R. Black, *IEEE Trans. Electron Devices* 16, 338 (1969).
8. J.D. Wu, P.J. Zheng, K. Lee, C.T. Chiu, and J.J. Lee, *Proc. 52nd Electronic Components and Technology Conference*, (Piscataway, NJ: IEEE, 2002), p. 452.
9. S.W. Liang, Y.W. Chang, and C. Chen, *J. Electron. Mater.* (in press).